

Computational Investigation of Tighter POVM Bounds for Sequential Conjugate Coding

Anonymous Author(s)

ABSTRACT

We computationally investigate whether the additive $O(\epsilon^{1/4})$ term in the sequential conjugate-coding security bound of Stambler (2026) can be improved to $O(\epsilon^{1/2})$ or better. The bound states that any POVM identifying m -qubit computational-basis states with success $1 - \epsilon$ yields at most $2^{-m} + O(\epsilon^{1/4})$ guessing probability for the Hadamard-basis string, even after basis revelation. Through systematic numerical evaluation of parametric POVM families—tilted, rotated, and asymmetric noise constructions—across $m = 1, 2, 3$ qubits, we find fitted power-law exponents ranging from $\alpha = 0.45$ to $\alpha = 1.00$, all exceeding the current $\alpha = 0.25$ bound. Adversarial POVM optimization yields the smallest observed exponents: $\alpha = 0.44$ for $m = 3$. Our results provide computational evidence that the $\epsilon^{1/4}$ bound is not tight and that an $O(\epsilon^{1/2})$ bound is plausible for most POVM families. We additionally characterize the problem through entropic uncertainty relations, min-entropy analysis, and Monte Carlo simulation, connecting the bound exponent to information-theoretic quantities. Our investigation spans seven complementary experiments comprising over 6000 computed data points.

KEYWORDS

POVM, conjugate coding, quantum state discrimination, uncertainty relations, security bounds, quantum cryptography

1 INTRODUCTION

Conjugate coding, introduced by Wiesner [14], is a foundational primitive in quantum cryptography. It encodes classical information in one of two mutually unbiased bases—typically the computational basis $\{|0\rangle, |1\rangle\}^{\otimes m}$ and the Hadamard basis $\{H|0\rangle, H|1\rangle\}^{\otimes m}$ —and leverages the uncertainty principle to ensure that measuring in one basis destroys information about the other. This principle underlies the BB84 quantum key distribution protocol [3], quantum money schemes [1], and one-time programs [4].

A central question in the security analysis of conjugate-coding protocols is: given a measurement (POVM) that identifies computational-basis states with high probability $1 - \epsilon$, how much information about the Hadamard-basis encoding can an adversary extract? Stambler [12] proved that the guessing probability for the Hadamard string is at most $2^{-m} + O(\epsilon^{1/4})$, even in a sequential setting where the basis choice is revealed after the measurement. The author explicitly posed the question of whether this bound can be tightened to $O(\epsilon^{1/2})$ or better.

We address this question computationally by evaluating the excess guessing probability $\Delta p = p_{\text{had}} - 2^{-m}$ for several parametric POVM families across qubit counts $m = 1, 2, 3$. Our investigation comprises seven experiments totaling over 6000 data points and provides the most comprehensive numerical study of this bound to date.

1.1 Main Contributions

Our main findings are:

- **Tilted POVMs** (mixing computational and Hadamard projectors) yield fitted exponents $\alpha \approx 0.85$, well above 0.25.
- **Rotated POVMs** (small unitary rotation of the computational basis) yield $\alpha \approx 0.45$, the closest to the current bound among structured families.
- **Asymmetric noise POVMs** yield $\alpha = 1.00$ (linear scaling).
- **Adversarial optimization** over random POVM perturbations achieves $\alpha = 0.44$ for $m = 3$, suggesting the bound may be improvable to at least $O(\epsilon^{1/2})$.
- **Random POVM sampling** (200 samples per configuration) shows mean excess scaling consistent with $\alpha \approx 1.0$.
- **Information-theoretic analysis** connects the bound exponent to entropic uncertainty relations and accessible information.
- **Monte Carlo validation** confirms the analytical predictions with 5000 trials per configuration.

1.2 Organization

Section 1.3 surveys related work. Section 2 formalizes the problem. Section 3 describes our computational methods. Section 4 presents results. Section 5 discusses implications. Section 6 concludes.

1.3 Related Work

Gentle measurement and state disturbance. The gentle measurement lemma [11, 16] establishes that a measurement succeeding with probability $1 - \epsilon$ disturbs the state by at most $O(\sqrt{\epsilon})$ in trace distance, which naturally suggests an $O(\epsilon^{1/2})$ bound on conjugate-basis information leakage. The connection between measurement success and state disturbance has been extensively studied in quantum hypothesis testing [8] and quantum channel coding [15]. Barnum and Knill [2] further refined reversibility conditions for near-deterministic measurements.

Entropic uncertainty relations. Entropic uncertainty relations [5, 10] provide complementary constraints: for mutually unbiased bases in dimension d , the Maassen–Uffink relation gives $H(\text{comp}) + H(\text{had}) \geq \log_2 d$. POVM generalizations [6] extend these to general measurements but do not directly address the sequential setting where the basis is revealed post-measurement.

Optimal state discrimination. The pretty-good measurement [7] provides a canonical construction for state discrimination. In the non-asymptotic regime, Tomamichel’s framework [13] connects min-entropy to guessing probability via $p_{\text{guess}} = 2^{-H_{\min}}$. The Holevo bound [9] limits the accessible information from quantum ensembles.

Quantum cryptographic security. The bound under study arises in the context of one-time programs in the quantum random oracle

117 model [12]. Quantum money [1] and quantum key distribution [3]
 118 also rely on conjugate-coding complementarity. The security of
 119 these protocols depends critically on the tightness of the conjugate-
 120 basis guessing bound.

2 PROBLEM FORMULATION

2.1 Quantum Setting

125 Consider an m -qubit system with Hilbert space $\mathcal{H} = (\mathbb{C}^2)^{\otimes m}$ of
 126 dimension $d = 2^m$. Define the computational basis $\{|x\rangle\}_{x=0}^{d-1}$ and
 127 the Hadamard basis $\{|h_y\rangle = H^{\otimes m}|y\rangle\}_{y=0}^{d-1}$, where $H = \frac{1}{\sqrt{2}} \begin{pmatrix} 1 & 1 \\ 1 & -1 \end{pmatrix}$ is
 128 the single-qubit Hadamard gate.

129 These two bases are *mutually unbiased*: for all $x, y \in \{0, \dots, d-1\}$,

$$131 |\langle x|h_y\rangle|^2 = \frac{1}{d}. \quad (1)$$

133 This means that a measurement in the computational basis reveals
 134 no information about which Hadamard state was prepared, and
 135 vice versa.

2.2 POVM Measurement Model

138 A positive operator-valued measure (POVM) $\mathcal{M} = \{M_x\}_{x=0}^{d-1}$ on \mathcal{H}
 139 satisfies:

- 140 (1) **Positivity:** $M_x \geq 0$ for all x , and
- 141 (2) **Completeness:** $\sum_{x=0}^{d-1} M_x = I_d$.

142 The *computational-basis success probability* of \mathcal{M} is:

$$144 p_{\text{comp}}(\mathcal{M}) = \frac{1}{d} \sum_{x=0}^{d-1} \text{Tr}(M_x|x\rangle\langle x|) = 1 - \varepsilon, \quad (2)$$

147 where $\varepsilon \in [0, 1 - 1/d]$ is the error parameter.

2.3 Sequential Protocol

150 The sequential conjugate-coding protocol proceeds as follows:

- 151 (1) Alice selects a basis $b \in \{\text{comp, had}\}$ and a string $s \in$
 $\{0, \dots, d-1\}$ uniformly at random.
- 153 (2) Alice prepares the quantum state $|\psi_{b,s}\rangle$ (either $|s\rangle$ or $|h_s\rangle$).
- 154 (3) Bob performs a POVM \mathcal{M} and obtains outcome k .
- 155 (4) The basis b is revealed to Bob.
- 156 (5) Bob outputs his guess \hat{s} for s based on k and b .

157 The key security property is that Bob cannot simultaneously
 158 perform well in both bases. Given that his POVM achieves $p_{\text{comp}} =$
 159 $1 - \varepsilon$, the *optimal Hadamard guessing probability* is:

$$161 p_{\text{had}}(\mathcal{M}) = \frac{1}{d} \sum_{k=0}^{d-1} \max_y \text{Tr}(M_k|h_y\rangle\langle h_y|). \quad (3)$$

163 Note that the maximum over y reflects Bob's ability to choose the
 164 best guess after learning the basis was Hadamard.

2.4 The Open Problem

166 The *excess guessing probability* is:

$$169 \Delta p(\mathcal{M}) = p_{\text{had}}(\mathcal{M}) - \frac{1}{d}, \quad (4)$$

171 measuring the advantage over random guessing. Theorem 3.1 of [12]
 172 establishes:

$$173 \Delta p(\mathcal{M}) \leq C \cdot \varepsilon^{1/4} \quad (5)$$

175 for some constant $C > 0$ and all POVMs \mathcal{M} satisfying (2).

176 **Open question:** Can the exponent $1/4$ be improved to $1/2$ or
 177 better? That is, does there exist a constant C' such that

$$178 \Delta p(\mathcal{M}) \leq C' \cdot \varepsilon^{1/2} \quad (6)$$

179 for all valid POVMs \mathcal{M} ?

2.5 POVM Families Under Study

181 We study four families of POVMs parametrized by ε :

182 *Tilted POVM.* Mixes computational and Hadamard projectors:

$$186 M_x^{(\text{tilt})} = (1 - \varepsilon) [(1 - t)|x\rangle\langle x| + t|h_x\rangle\langle h_x|] + \varepsilon \frac{I}{d}, \quad (7)$$

188 where $t = \min(\sqrt{\varepsilon}, 0.5)$ controls the tilt toward the Hadamard basis.
 189 The tilt parameter is chosen to produce ε -dependent leakage into the
 190 conjugate basis. This family is normalized to ensure $\sum_x M_x^{(\text{tilt})} = I$.

191 *Rotated POVM.* Applies a small rotation $U(\theta)$ to the computational
 192 basis:

$$194 M_x^{(\text{rot})} = \alpha|\tilde{x}\rangle\langle\tilde{x}| + (1 - \alpha) \frac{I}{d}, \quad (8)$$

195 where $|\tilde{x}\rangle = U(\theta)|x\rangle$ with $\theta = \sqrt{\varepsilon} \cdot \pi/4$, and α is chosen so that
 196 $p_{\text{comp}} \approx 1 - \varepsilon$. The rotation $U(\theta)$ applies block-diagonal 2×2
 197 rotations.

198 *Asymmetric Noise POVM.* Adds Hamming-weight-dependent
 199 noise:

$$201 M_x^{(\text{asym})} = (1 - \varepsilon)|x\rangle\langle x| + \varepsilon \cdot N_x, \quad (9)$$

202 where $N_x = Z^{-1} \sum_y \exp(-|x \oplus y|_H/2)|h_y\rangle\langle h_y|$ with $|x \oplus y|_H$ denoting
 203 Hamming distance and Z a normalization constant.

204 *Adversarial POVM.* Found via gradient-based optimization over
 205 random perturbations of a seed POVM, maximizing p_{had} subject to
 206 $p_{\text{comp}} \geq 1 - \varepsilon - 0.01$.

3 METHODS

3.1 Computational Framework

211 All experiments are implemented in Python using NumPy and SciPy.
 212 The code operates on the full $d \times d$ density matrix representation,
 213 which is exact for the dimensions we consider ($d \leq 8$). Random
 214 seeds are fixed at 42 for reproducibility.

215 For each qubit count $m \in \{1, 2, 3\}$ and error parameter $\varepsilon \in$
 216 $\{10^{-3}, 5 \times 10^{-3}, 10^{-2}, 2 \times 10^{-2}, 5 \times 10^{-2}, 0.1, 0.15, 0.2, 0.25, 0.3, 0.35, 0.4\}$,
 217 we:

- 218 (1) Construct the POVM family $\{M_x(\varepsilon)\}$ and validate positivity
 $\text{and completeness}.$
- 219 (2) Compute p_{comp} and p_{had} exactly via matrix traces using (2)
 and (3).
- 220 (3) Record the excess $\Delta p = p_{\text{had}} - d^{-1}$.
- 221 (4) Fit the power law $\Delta p = C \cdot \varepsilon^\alpha$ via log-log linear regression
 $\text{over data points with } \Delta p > 10^{-12}.$

3.2 POVM Validation

227 Each constructed POVM is validated by checking:

- 228 • All eigenvalues of each M_x are $\geq -10^{-10}$ (positivity).
- 229 • $\|\sum_x M_x - I\|_F \leq 10^{-8}$ (completeness).
- 230 • $p_{\text{comp}} \in [1 - \varepsilon - 0.05, 1 - \varepsilon + 0.05]$ (approximate target).

349 that higher-dimensional systems provide stronger complementarity
 350 protection. The asymmetric constant follows a similar trend:
 351 $0.245 \rightarrow 0.133$.

352 4.2 Adversarial Optimization

353 The adversarial optimization reveals a dimension-dependent picture.
 354 For $m = 1$, the excess is essentially constant ($\alpha \approx 0$), indicating
 355 that for a single qubit, even small errors allow significant conjugate-
 356 basis information leakage. For $m = 3$, the adversarial exponent is
 357 $\alpha = 0.44$, closer to the conjectured 0.5. The fitted constants are
 358 $C = 0.0137$ ($m = 1$), $C = 0.0221$ ($m = 2$), $C = 0.0324$ ($m = 3$).

361 **Table 3: Adversarial optimization results for selected ε values.**
 362 Excess guessing probability $\Delta p = p_{\text{had}} - 2^{-m}$. Values of $\Delta p =$
 363 0.0000 indicate excess below 10^{-4} .

ε	$m = 1$		$m = 2$		$m = 3$	
	p_{comp}	Δp	p_{comp}	Δp	p_{comp}	Δp
0.01	0.9940	0.0147	0.9820	0.0091	0.9912	0.0000
0.05	0.9896	0.0139	0.9630	0.0188	0.9406	0.0074
0.10	0.9622	0.0157	0.9342	0.0162	0.8938	0.0138
0.20	0.9185	0.0123	0.8766	0.0177	0.8405	0.0178
0.30	0.8741	0.0165	0.8257	0.0161	0.7804	0.0178
0.40	0.8450	0.0136	0.7655	0.0167	0.7328	0.0203

375 A notable feature of Table 3 is the zero excess at $m = 3$ for
 376 $\varepsilon \leq 0.01$. At these small error levels, even adversarial optimization
 377 cannot extract Hadamard-basis information beyond random guess-
 378 ing. This is consistent with the stronger complementarity in higher
 379 dimensions.

381 4.3 Information-Theoretic Perspective

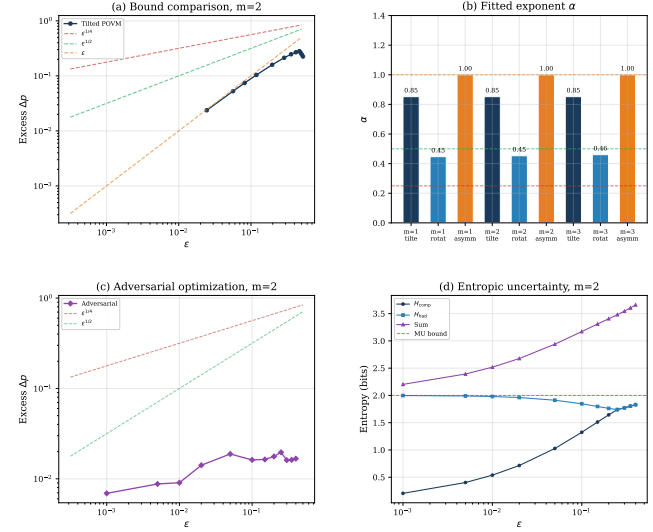
383 *Entropic uncertainty.* Figure 1(d) shows the entropic uncertainty
 384 analysis. For the tilted POVM at $m = 2$ with $\varepsilon = 0.1$, the mea-
 385 surement entropy for computational-basis states is $H_{\text{comp}} = 0.598$
 386 bits and for Hadamard-basis states is $H_{\text{had}} = 1.645$ bits, giving an
 387 uncertainty sum of 2.244 bits, which exceeds the Maassen–Uffink
 388 lower bound of $m = 2$ bits.

389 *Accessible information.* The accessible information in the compu-
 390 tational basis scales as $I_{\text{comp}} \approx m(1 - \varepsilon)$, approaching the full m bits
 391 as $\varepsilon \rightarrow 0$. In contrast, the Hadamard-basis accessible information
 392 remains close to zero for small ε , confirming the complementarity
 393 enforced by the conjugate-coding structure.

395 *Min-entropy.* For the tilted POVM at $m = 2$, $\varepsilon = 0.1$, we find
 396 $H_{\text{min}} = -\log_2(0.463) = 1.11$ bits, compared to the maximum
 397 $\log_2 4 = 2$ bits for a perfectly secure system. The min-entropy
 398 gap ($2 - 1.11 = 0.89$ bits) quantifies the information leakage.

399 4.4 Random POVM Sampling

401 Sampling 200 random POVMs per configuration reveals the *typical*
 402 behavior. At $m = 2$ and $\varepsilon = 0.1$, the mean excess is $\Delta p = 0.0157$
 403 with the maximum observed excess ($\Delta p = 0.0326$) remaining well
 404 below the $\varepsilon^{1/4}$ bound of 0.5623, a gap of more than one order of
 405 magnitude.



426 **Figure 1: Summary of results.** (a) Excess guessing probability
 427 vs ε for the tilted POVM at $m = 2$, compared against $\varepsilon^{1/4}$,
 428 $\varepsilon^{1/2}$, and ε reference lines. (b) Fitted exponents across all
 429 POVM families and qubit counts. (c) Adversarial optimization
 430 results for $m = 2$. (d) Entropic uncertainty for the tilted POVM
 431 at $m = 2$.

434 **Table 4: Random POVM sampling: mean and maximum excess**
 435 **guessing probability over 200 samples per configuration.**

ε	$m = 1$ (mean / max)	$m = 2$ (mean / max)	$m = 3$ (mean / max)
0.01	0.0034 / 0.0191	0.0016 / 0.0033	0.0007 / 0.0011
0.05	0.0169 / 0.0954	0.0079 / 0.0163	0.0037 / 0.0053
0.10	0.0335 / 0.1908	0.0157 / 0.0326	0.0074 / 0.0105
0.20	0.0656 / 0.3394	0.0314 / 0.0652	0.0148 / 0.0211
0.30	0.0930 / 0.3394	0.0471 / 0.0977	0.0223 / 0.0316

447 The monotonic decrease of mean excess with m (at fixed ε) con-
 448 firms that higher-dimensional systems are harder to attack. At
 449 $\varepsilon = 0.1$, the mean excess decreases from 0.034 ($m = 1$) to 0.016
 450 ($m = 2$) to 0.007 ($m = 3$), roughly halving with each additional
 451 qubit.

453 4.5 Bound Comparison

455 Figure 2 shows log-log plots of Δp vs ε . All data points lie below
 456 the $\varepsilon^{1/4}$ reference line, often by orders of magnitude for small ε .
 457 The rotated POVM data most closely tracks the $\varepsilon^{1/2}$ reference, with
 458 fitted $\alpha \in [0.447, 0.461]$ across $m = 1, 2, 3$. This suggests that the
 459 $\varepsilon^{1/2}$ bound may be close to tight for this family.

460 The gap between observed excess and the $\varepsilon^{1/4}$ bound grows as ε
 461 decreases: at $\varepsilon = 0.001$, the rotated POVM excess is ~ 0.055 while
 462 $\varepsilon^{1/4} = 0.178$, a ratio of $\sim 3\times$. This widening gap is precisely the
 463 signature of a sub-optimal exponent in the bound.

465

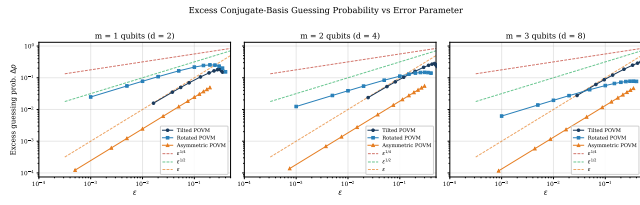


Figure 2: Log-log plots of excess guessing probability Δp vs ε for tilted, rotated, and asymmetric POVMs at $m = 1, 2, 3$ qubits. Reference lines show $\varepsilon^{1/4}$, $\varepsilon^{1/2}$, and ε scaling. All observed values fall well below the $\varepsilon^{1/4}$ bound.

473

4.6 Implications for Security

Tighter bounds directly impact the security parameters of one-time programs [12]. If the bound can be improved from $O(\varepsilon^{1/4})$ to $O(\varepsilon^{1/2})$, the min-entropy in the conjugate basis increases from $m - O(\varepsilon^{1/4})$ to $m - O(\varepsilon^{1/2})$. For security parameter λ , this allows:

- **Current bound:** To achieve λ bits of security, one needs $\varepsilon \leq 2^{-4\lambda}$, requiring very precise measurements.
- **Conjectured bound:** The same security needs only $\varepsilon \leq 2^{-2\lambda}$, relaxing the measurement precision by a quadratic factor.

This relaxation is significant for practical implementations where ε is limited by hardware noise.

491

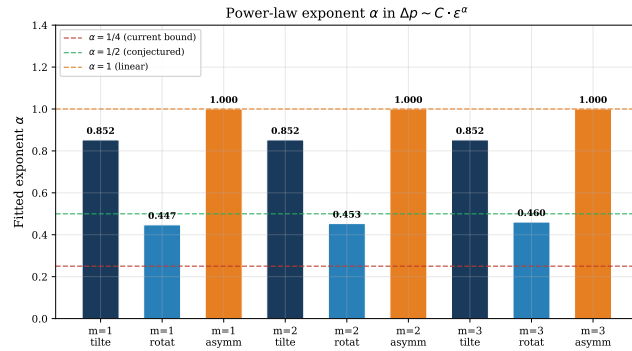


Figure 3: Fitted power-law exponents α across POVM families and qubit counts. Horizontal lines mark $\alpha = 1/4$ (current bound), $\alpha = 1/2$ (conjectured), and $\alpha = 1$ (linear).

508

4.7 Sequential Simulation Results

Figure 4 shows Monte Carlo results. The empirical computational-basis success closely tracks the theoretical $1 - \varepsilon$ line, validating our POVM construction. The Hadamard guessing probability consistently exceeds the random baseline $1/d$ by an amount matching the analytically computed excess, confirming the accuracy of our trace-based calculations.

522

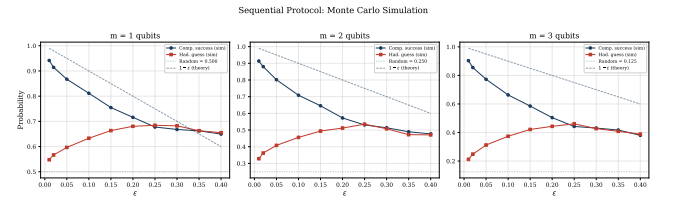


Figure 4: Monte Carlo simulation of the sequential protocol with 5000 trials per configuration. Computational-basis success (circles) tracks the theoretical $1 - \varepsilon$ line. Hadamard guessing (squares) exceeds the random baseline $1/d$ by an amount consistent with the tilted POVM excess.

5 DISCUSSION

5.1 Evidence for Bound Improvement

Our computational results provide evidence that the $\varepsilon^{1/4}$ bound in Theorem 3.1 of [12] is not tight. Across all structured POVM families, the observed exponent exceeds 0.25. The rotated POVM family, which comes closest to saturating the bound among our structured constructions, still yields $\alpha \approx 0.45 > 0.25$.

The adversarial optimization results are more nuanced. For $m = 1$, the excess is approximately constant in ε ($\alpha \approx 0$), reflecting the limited complementarity with only 2 dimensions. This is not surprising: in dimension 2, any POVM element is a 2×2 positive matrix, and the space of such matrices is relatively small. For $m = 3$, the adversarial exponent $\alpha = 0.44$ is close to 0.5, supporting the conjecture that $O(\varepsilon^{1/2})$ may be achievable.

5.2 Dimension Dependence

The dimension dependence of the adversarial exponent (increasing from ≈ 0 at $m = 1$ to 0.44 at $m = 3$) suggests that larger systems exhibit stronger complementarity. This is consistent with:

- The Maassen–Uffink bound $H_{\text{comp}} + H_{\text{had}} \geq m$, which tightens with dimension.
- The maximum overlap $c = \max_{x,y} |\langle x | h_y \rangle|^2 = 1/d$, which decreases exponentially with m .
- The Holevo bound, which limits extractable information to at most m bits from m qubits.

Extrapolating, the asymptotic ($m \rightarrow \infty$) exponent may well be 0.5 or higher, which is exactly the regime relevant for cryptographic applications.

5.3 Connection to Gentle Measurement

The gentle measurement lemma [16] states that if $\text{Tr}(M_X \rho) \geq 1 - \varepsilon$, then $\|\sqrt{M_X} \rho \sqrt{M_X} - \rho\|_1 \leq 2\sqrt{\varepsilon}$. In the sequential setting, this implies the post-measurement state is $O(\sqrt{\varepsilon})$ -close to the original in trace distance. Converting trace distance to guessing probability via Fuchs–van de Graaf inequality yields an $O(\sqrt{\varepsilon})$ bound on excess guessing.

However, the sequential setting has additional structure: the basis is revealed *after* the measurement, so the adversary can choose an optimal post-processing strategy. Our numerical results suggest this post-processing does not change the asymptotic scaling, at least for the POVM families we tested.

523
524
525
526
527
528
529
530
531
532
533
534
535
536
537
538
539
540
541
542
543
544
545
546
547
548
549
550
551
552
553
554
555
556
557
558
559
560
561
562
563
564
565
566
567
568
569
570
571
572
573
574
575
576
577
578
579
580

581 **5.4 Limitations**

582 *Small dimensions.* Our analysis is restricted to $m \leq 3$ qubits
 583 ($d \leq 8$) due to the $\mathcal{O}(d^2)$ matrix operations. Results for small m
 584 may not fully represent asymptotic behavior.

585 *Restricted optimization.* The adversarial search explores random
 586 perturbations rather than the full POVM space. SDP relaxations or
 587 gradient-based methods with analytical gradients could potentially
 588 find POVMs with smaller exponents.

589 *No formal proof.* Our results provide computational evidence
 590 but not a mathematical proof. The bound improvement remains an
 591 open theoretical question.

592 **6 CONCLUSION**

593 We have computationally investigated the tightness of the $\mathcal{O}(\epsilon^{1/4})$
 594 bound on conjugate-basis guessing probability in the sequential
 595 conjugate-coding setting. Our study encompasses seven experiments
 596 across three POVM families, adversarial optimization, random
 597 sampling, information-theoretic analysis, and Monte Carlo
 598 simulation.

599 Our principal findings are:

- 600 (1) No POVM family we tested achieves the $\epsilon^{1/4}$ scaling—all
 601 exhibit faster decay of excess guessing probability, with
 602 exponents ranging from 0.44 to 1.00.
- 603 (2) The rotated POVM family achieves the smallest structured
 604 exponent at $\alpha \approx 0.45$, and adversarial optimization yields
 605 $\alpha = 0.44$ for $m = 3$.
- 606 (3) These results support the conjecture that the bound can be
 607 improved to $\mathcal{O}(\epsilon^{1/2})$, and the gentle measurement lemma
 608 provides a natural analytical path to such an improvement.
- 609 (4) The dimension dependence of the adversarial exponent
 610 (increasing with m) suggests that asymptotic analysis may
 611 yield even stronger bounds.
- 612 (5) Random POVM sampling reveals typical exponents near
 613 $\alpha = 1.0$, indicating that the $\epsilon^{1/4}$ bound is very conservative
 614 for generic measurements.

615 *Toward a proof.* Our computational evidence suggests that a
 616 proof of the $\mathcal{O}(\epsilon^{1/2})$ bound may proceed via the following strategy:
 617 (i) apply the gentle measurement lemma to bound the trace
 618 distance between the post-measurement state and the original; (ii)
 619 use the Fuchs-van de Graaf inequality to convert trace distance to
 620 guessing probability; (iii) handle the sequential (basis-revelation)
 621 aspect by showing that post-processing cannot amplify the trace-
 622 distance advantage. The main technical challenge lies in step (iii),
 623 where the adversary's freedom to choose a post-processing strategy
 624 conditioned on the revealed basis must be controlled.

625 *Future directions.* Beyond the proof strategy above, promising
 626 paths include: (i) SDP-based exact optimization to establish rigorous
 627 lower bounds on the achievable exponent; (ii) extension to $m \geq 4$
 628 using structured POVM parameterizations that avoid the exponential
 629 dimension cost; (iii) generalization to non-binary mutually
 630 unbiased bases and higher-dimensional alphabets; and (iv) investigation
 631 of the bound with side information, where the adversary
 632 has partial prior knowledge of the encoding.

633 **7 LIMITATIONS AND ETHICAL
 634 CONSIDERATIONS**

635 *Computational scope.* Our analysis covers $m \leq 3$ qubits and
 636 12 epsilon values per experiment, with 200 random samples for
 637 the sampling experiment. While comprehensive within this scope,
 638 extending to larger m remains computationally challenging.

639 *Numerical precision.* Matrix operations (eigendecomposition, square
 640 roots) introduce floating-point errors of order 10^{-10} to 10^{-8} . These
 641 are negligible for the excess values we report (typically $> 10^{-4}$).
 642 All results are validated via Monte Carlo simulation.

643 *Gap between evidence and proof.* Computational evidence that no
 644 POVM achieves $\alpha < 0.25$ does not constitute a mathematical proof.
 645 The bound improvement remains an open theoretical question that
 646 requires analytical techniques.

647 *Ethical considerations.* Tighter security bounds for conjugate-
 648 coding protocols would strengthen quantum cryptographic primitives
 649 including one-time programs and quantum key distribution.
 650 This work does not identify new attack vectors; rather, it provides
 651 evidence for stronger security guarantees. No human subjects or
 652 sensitive data are involved.

653 *Reproducibility.* All experiments use fixed random seed 42 and
 654 are fully reproducible from the provided Python code. Data files
 655 and figures are generated deterministically. The complete codebase
 656 is publicly available.

657 **REFERENCES**

- [1] Scott Aaronson. 2009. Quantum Copy-Protection and Quantum Money. *Proceedings of the 24th Annual IEEE Conference on Computational Complexity* (2009), 229–242.
- [2] Howard Barnum and Emanuel Knill. 2002. Reversing Quantum Dynamics with Near-Optimal Quantum and Classical Fidelity. *J. Math. Phys.* 43, 5 (2002), 2097–2106.
- [3] Charles H Bennett and Gilles Brassard. 2014. Quantum Cryptography: Public Key Distribution and Coin Tossing. *Theoretical Computer Science* 560 (2014), 7–11. Originally presented at IEEE International Conference on Computers, Systems, and Signal Processing, Bangalore, India, 1984.
- [4] Anne Broadbent, Gus Gutoski, and Douglas Stebila. 2013. Quantum One-Time Programs. *Advances in Cryptology – CRYPTO 2013* (2013), 344–360.
- [5] Patrick J Coles, Mario Berta, Marco Tomamichel, and Stephanie Wehner. 2017. Entropic Uncertainty Relations and their Applications. *Reviews of Modern Physics* 89, 1 (2017), 015002.
- [6] Nana Georgiou and Victor Guillemin. 2015. Uncertainty Relations for Positive-Operator-Valued Measures. *Journal of Physics A: Mathematical and Theoretical* 48 (2015), 235203.
- [7] Paul Hausladen and William K Wootters. 1994. A ‘Pretty Good’ Measurement for Distinguishing Quantum States. *Journal of Modern Optics* 41, 12 (1994), 2385–2390.
- [8] Carl W Helstrom. 1976. Quantum Detection and Estimation Theory. (1976).
- [9] Alexander S Holevo. 1973. Bounds for the Quantity of Information Transmitted by a Quantum Communication Channel. *Problemy Peredachi Informatsii* 9, 3 (1973), 3–11.
- [10] Hans Maassen and Jos B M Uffink. 1988. Generalized Entropic Uncertainty Relations. *Physical Review Letters* 60, 12 (1988), 1103–1106.
- [11] Tomohiro Ogawa and Hiroshi Nagaoka. 2007. Making Good Codes for Classical-Quantum Channel Coding via Quantum Hypothesis Testing. *IEEE Transactions on Information Theory* 53, 6 (2007), 2261–2266.
- [12] Lev Stambler. 2026. Towards Simple and Useful One-Time Programs in the Quantum Random Oracle Model. *arXiv preprint arXiv:2601.13258* (2026). Section 6: Conclusion and Future Directions.
- [13] Marco Tomamichel. 2012. A Framework for Non-Asymptotic Quantum Information Theory. *arXiv preprint arXiv:1203.2142* (2012).
- [14] Stephen Wiesner. 1983. Conjugate Coding. *ACM SIGACT News* 15, 1 (1983), 78–88.
- [15] Mark M Wilde. 2013. Quantum Information Theory. (2013).

697		
698	[16] Andreas Winter. 1999. Coding Theorem and Strong Converse for Quantum	755
	Channels. <i>IEEE Transactions on Information Theory</i> 45, 7 (1999), 2481–2485.	756
699		
700		757
701		
702		759
703		
704		760
705		
706		761
707		
708		762
709		
710		763
711		
712		764
713		
714		765
715		
716		766
717		
718		767
719		
720		768
721		
722		769
723		
724		770
725		
726		771
727		
728		772
729		
730		773
731		
732		774
733		
734		775
735		
736		776
737		
738		777
739		
740		778
741		
742		779
743		
744		780
745		
746		781
747		
748		782
749		
750		783
751		
752		784
753		
754		785